

PAPER

Bioinspired locomotion and grasping in water: the soft eight-arm OCTOPUS robot

To cite this article: M Cianchetti *et al* 2015 *Bioinspir. Biomim.* **10** 035003

View the [article online](#) for updates and enhancements.

Related content

- [Dynamics of underwater legged locomotion: modeling and experiments on an octopus-inspired robot](#)
M Calisti, F Corucci, A Arienti et al.
- [An octopus-bioinspired solution to movement and manipulation for soft robots](#)
M Calisti, M Giorelli, G Levy et al.
- [Soft-robotic arm inspired by the octopus: II. From artificial requirements to innovative technological solutions](#)
B Mazzolai, L Margheri, M Cianchetti et al.

Recent citations

- [Temporal and spatial programming in soft composite hydrogel objects](#)
Ross W. Jaggers and Stefan A. F. Bon
- [Mariangela Manti *et al*](#)
- [An Additive Millimeter-Scale Fabrication Method for Soft Biocompatible Actuators and Sensors](#)
Sheila Russo *et al*

Bioinspiration & Biomimetics



RECEIVED
15 April 2014

REVISED
26 August 2014

ACCEPTED FOR PUBLICATION
1 September 2014

PUBLISHED
13 May 2015

SPECIAL ISSUES/SECTIONS

Bioinspired locomotion and grasping in water: the soft eight-arm OCTOPUS robot

M Cianchetti¹, M Calisti¹, L Margheri¹, M Kuba² and C Laschi¹

¹ The BioRobotics Institute, Scuola Superiore Sant'Anna, Viale Rinaldo Piaggio 34, I-56025 Pontedera (Pisa), Italy

² Department of Neurobiology, Hebrew University of Jerusalem, Jerusalem, Israel

E-mail: matteo.cianchetti@sssup.it

Keywords: soft robotics, octopus, biomimetics

Abstract

The octopus is an interesting model for the development of soft robotics, due to its high deformability, dexterity and rich behavioural repertoire. To investigate the principles of octopus dexterity, we designed an eight-arm soft robot and evaluated its performance with focused experiments. The OCTOPUS robot presented here is a completely soft robot, which integrates eight arms extending in radial direction and a central body which contains the main processing units. The front arms are mainly used for elongation and grasping, while the others are mainly used for locomotion. The robotic octopus works in water and its buoyancy is close to neutral. The experimental results show that the octopus-inspired robot can walk in water using the same strategy as the animal model, with good performance over different surfaces, including walking through physical constraints. It can grasp objects of different sizes and shapes, thanks to its soft arm materials and conical shape.

1. Introduction

The octopus is a cephalopod mollusc, an invertebrate living in most oceans and seas. Its body has eight identical arms and no rigid parts, and is mostly composed of muscular tissues. The special morphology of the body, the high dexterity provided by the shape and tissues of the arms and their efficient neural control mechanisms provide the octopus with a rich repertoire of movements and behaviours: the octopus has reaching and grasping capabilities, locomotion via crawling and swimming, camouflage abilities and smart strategies for hunting and hiding. The octopus is paradigmatic biological case of how effective behaviour is strictly related to the body's morphology and to interaction with the environment. It represents a very interesting model for robotics for a number of reasons: its arms are continuum structures with no rigid skeletons, bending in all directions, at any point along the arm length, hence providing an infinite number of degrees of freedom; the arms can shorten and elongate and the full body can greatly deform to adapt to physical constraints; arm stiffness can be controlled and increased when forces need to be applied by the animal to the environment; and the arms can also perform grasping and locomotion.

The objective of this work was to design and develop an octopus-inspired robot, implementing the key principles of octopus dexterity and its main movements and behaviours.

The muscular structure of the octopus arm is also well known: a *muscular hydrostat* (Smith and Kier 1989) which is an isovolumetric structure composed almost entirely of tightly packed muscles fibres, arranged into transverse, longitudinal and oblique muscles (Sumbre *et al* 2001). The selective contractions of transverse and longitudinal muscles allow bending and elongation/shortening, co-contractions allow stiffening, while contractions of oblique muscles allow torsions. Additional insights on the anatomy, neurophysiology and biomechanics of the octopus arms were searched for purposively, in order to derive quantitative specifications for the design of the robot (Mazzolai *et al* 2012). Another biological insight which steered the engineering design regards the octopus' preferential use of its arms: in accordance with biological studies, the arms of the octopus are identical and do not show specializations or specialized use (Mather 1998). Nonetheless, octopuses prefer to use different arms for different tasks (Byrne *et al* 2006a, 2006b). For example, R1 and L1 are more frequently used for reaching, fetching, grasping,

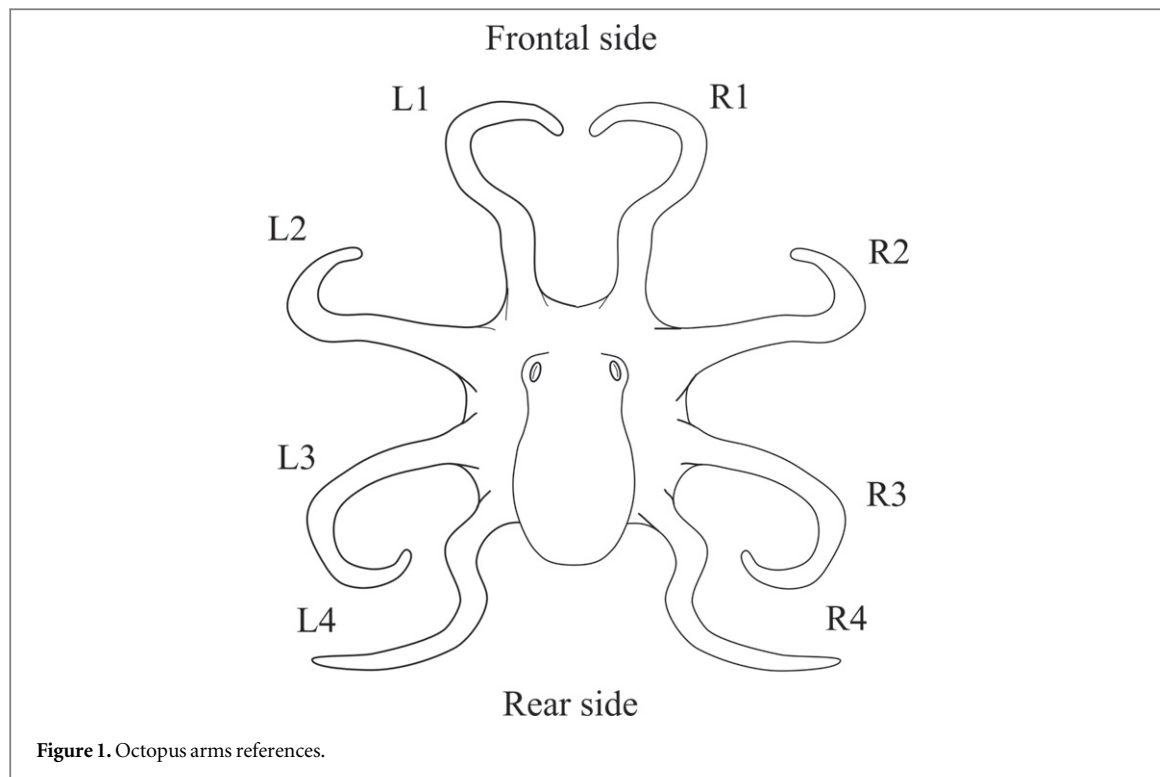


Figure 1. Octopus arms references.

sensing, while R2 to R4 and L3 to L4 are more frequently used for crawling and standing (figure 1). Moreover, it has been observed (unpublished data) that the octopus prefers using the medial part of the arms for grasping objects thus leading to important suggestions for robot sensorization and locomotion strategies.

When moving over a substrate, the octopus puts in place a mechanism by which some of the arms are used as sort of legs, which is referred to as crawling. Interestingly, the arms used are commonly a couple of back arms, which push the body forward, thanks to the neutral buoyancy of the octopus, allowing the body to be kept raised from the ground. The octopus pushes using the arm opposite to the direction of locomotion and the pulling arms do not contribute to the animal's movement (Levy and Hochner 2010, 2013). To change direction, octopuses do not use gaits similar to other legged animals, such as paddle-like movements or coordinated movements (Hirose *et al* 1986), but they simply change the arms involved in the pushing motion. The resulting direction of locomotion, therefore, is a vectorial combination of the arms used for pushing (Calisti *et al* 2011). Moreover, it has been found that pushing implies a stereotyped set of actions, that is a shortening of the proximal part, the attachment of the suckers to the substrate, the elongation of the proximal part and finally the detachment of the suckers. In living octopuses, the stereotyped movement of the arms is obtained with a sequence of actions which involves the coordination and contraction of several muscles.

The octopus-inspired robot presented here, OCTOPUS, is a completely soft robot, which

integrates eight arms extending in radial direction and a central body which contains the main processing units. The front arms are mainly used for manipulation, elongation and grasping, while the others are primarily used for locomotion. To optimize elongation, reaching and manipulation tasks, the front arms are inspired to the muscular hydrostat structure. The arm functional units were designed and developed resembling its fundamental elements: the absence of rigid structures, replication of the arm's morphology and shape, and arrangement of the muscles in longitudinal and transverse directions (Laschi *et al* 2009). Despite very advantageous from a robotic view point, the property of isovolumetric deformations was not replicated in the robotic arms since the amount of actuators needed to guarantee a spatially continuous deformation of a soft bodied arm is unapproachable. The motion mechanism was instead achieved exploiting the features of the supporting structure reported in the mechanical hardware description. The other arms, which are used for crawling, are based on silicone and cables, embedding the features needed to obtain octopus-inspired locomotion. The robotic octopus works in water and its buoyancy is close to neutral.

To the authors' knowledge, no previous works in literature have focused on the development of an underwater robot with both manipulation and legged locomotion capabilities, however, some references can be provided regarding studies that treat them separately.

A very large number of manipulators could be mentioned as previous attempts. Recalling all of them is out of the scope of the present work, but if we take into consideration only continuum and bioinspired

manipulators, only a few works remain: two robots inspired by the elephant trunk were presented at Clemson University, the elephant trunk based on prismatic joints actuated by cables (Walker 2000) and the OCTARM which is based on a series of pneumatic actuators (Walker *et al* 2005), both capable of reproducing elephant trunk behaviour and the latter recently used to climb structures (Walker *et al* 2012); the FESTO Bionic Handling was developed on the same basic idea, exploiting pneumatic actuators arranged in parallel and serial manner; the OCRobotics Snake Arm is an example of octopus-inspired manipulator which again uses tendons to orient a series of parallel rigid endplates (Walker 2013, Webster and Jones 2010)- an extensive and exhaustive overview regarding the design and control of continuum robots is reported). In this context, soft-material based robots represent a new trend: soft robots are devices which can actively interact with the environment and which can undergo ‘large’ deformations relying on inherent or structural compliance³. This results in the introduction of new technologies capable of exploiting structural or material properties to improve dexterity and manipulation capabilities. Examples and perspectives regarding soft robotics can be found in Trivedi *et al* (2008) and Laschi and Cianchetti (2014). If we add soft-material based robots to this selection, it is worth mentioning the jammable robot (by MIT) which combines a cable-driven actuation with the capability of changing its stiffness (Cheng *et al* 2012), the Harvard tentacle-like robots capable of large deformation generated by the pressurization of an embedded pneumatic chamber network (Martinez *et al* 2013) and the octopus-inspired robots developed by the authors of the present work where the combination of soft materials and a cable-driven transmission make it possible to accomplish manipulation (Cianchetti *et al* 2011).

As far as underwater legged locomotion is concerned, literature presents very few examples: among them, one of the most advanced is called Crabster200 (CR200) (Shim *et al* 2013), a hexapedal robot inspired by the crab, an octopus-inspired robot featuring elastic arms, developed by the authors (Calisti *et al* 2011) and a lobster inspired robotic platform (Ayers and Witting 2007). The first robot employs proper insulated legs with three degrees of freedom; it relies on hard material and it was designed for seabed exploration. In the second work, the robot mimics the crawling locomotion of the *Octopus vulgaris* by synthesizing mechanical and control aspects. It implements a pushing-based locomotion strategy enabling an omnidirectional robot motion, translating the center of mass from one position to another in a quasi-static

condition that alternates pushing phases with recovery phases. Finally, the latter work on lobsters focuses on the control strategy of underwater locomotion, implementing a biomimetic control for underwater walking. Terrestrial locomotion is a much more investigated field which counts several valuable works, but again, only the robotic platforms based on soft mechatronics technologies will be reported. There are examples of walking robots built from scratch which rely on continuum legs (Godage *et al* 2012) or soft legs (Shepherd *et al* 2011) to push themselves forward. Alternative bioinspired strategies for making soft robots move over a substrate have commonly been employed: rolling robots using different technologies such as the jamming phenomenon (Steltz *et al* 2009, Onal and Rus 2012); jumping robots based on shape memory alloys (SMAs) actuators (Lin *et al* 2011, Sugiyama and Hirai 2004); tendon-driven robots which rely on braided structures to implement peristaltic locomotion (Seok *et al* 2010). Specific mention should be made to the bioinspired salamander robot, which was extensively used to study the control of the swimming phase (in water) and walking phase (outside water) of a biological salamander (Crespi and Ijspeert 2008, Crespi *et al* 2013).

After the description of the OCTOPUS robot (section 2), this paper will present the experimental trials together with a detailed description of the methodologies used during the tests (section 3). These results will be reported (section 4) and discussed in detail from a technological and biological point of view (section 5). Finally conclusions and some remarks are provided (section 6).

2. The OCTOPUS robot

The robotic octopus integrates eight arms extending in radial direction and a central body (figure 2). It combines grasping and locomotion capabilities exploiting different technological solutions developed for actuation, sensing and control. All of the arms are connected to the base of the central body which contains the electrical and mechanical components needed on board to control the movement of the arms during manipulation and to implement robot locomotion concurrently. A detailed sketch describing all the components of the robotic arm is reported in figure 2 (left) and described in detail in the subsequent sections, while a picture of the real prototype is shown in figure 2 (right).

2.1. Mechanical bodyware

Biological insights into preferential use by the octopus of its arms led to designing the eight arms of the OCTOPUS artefact with different functional specializations, taking into account various structural differences with a view to optimizing their performance based on the specific task. This led to developing two

³ Definition agreed at the first plenary meeting of the RoboSoft Coordination Action—‘A Coordination Action for Soft Robotics’, funded by the European Commission in the ICT-FET Programme under contract #619319.

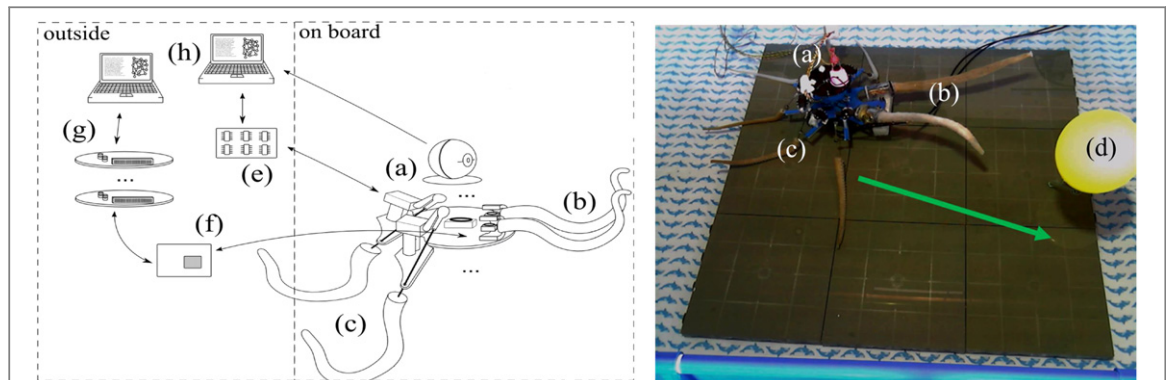


Figure 2. Sketch of the OCTOPUS robot: body with camera (a), manipulation arms (b), locomotion arms (c), the target balloon (d), locomotion arms driver board (e), current sensors, amplifiers and filters (f), manipulation control boards (g), computers which run the control architecture (h). The OCTOPUS prototype moving in the experimental area: the arrow represents the direction of locomotion.

different kinds of arms: one optimized for locomotion and one specialized in manipulation. They were designed following two different approaches: the manipulation arms were based on a morphological replication of the functional elements constituting the octopus' arms (namely the muscular hydrostat components); the locomotion arms relied on a functional synthesis derived from the natural counterpart while implementing crawling locomotion.

By referring to figures 1 and 2, the corresponding R1 and L1 arms of the OCTOPUS robot are devoted to manipulation and are able to elongate, shorten, bend in any direction, and vary stiffness. To optimize these capabilities, the frontal arms are equipped with motor-driven cable actuators and SMA actuators. SMAs are alloys that 'remember' their annealed shape and return to this shape only when heated. Springs made of SMA wire thus would contract from a stretched condition to the initial length upon heating. These materials still present several drawbacks, but since they are lightweight, compact and have very high power density, they are often considered as an alternative to conventional actuators (especially in soft robotics) (Cianchetti 2013).

In order to reproduce the *O. vulgaris* manipulation capabilities, equivalent artificial muscular hydrostat units were reproduced using SMA springs as reported in Follador *et al* (2012). Their combination led to the fabrication of a soft continuum manipulator, working in water (Cianchetti *et al* 2014). Although a complete and detailed description of the octopus-like robotic arm can also be found in Laschi *et al* (2012), the main characteristics will be reported here for the reader's convenience. The arm actuation system is based on longitudinal and transverse SMA spring units and a motor-driven cable. In order to transmit and propagate the local action of the actuators, they were internally connected to a soft and flexible braided sleeve, working as an overall supporting structure. This structure is made of braided polyethylene threads (similar to what is used in McKibben actuators) and is highly

flexible. At the same time it has the double role of supporting the actuators and transmitting forces from transversal direction to longitudinal and vice-versa (mimicking the muscular hydrostat's behaviour, despite not following an isovolumetric law).

A layer of skin covers the whole structure and components, insulating them from the water environment. Its thickness (less than 1 mm) is the result of the best compromise between mechanical robustness (essential for insulation) and the attempt to reduce interferences during arm movements. A cylindrical base houses a dc motor dedicated to the actuation of the cable (that is fastened at the tip, passing inside the arm) and gathers all the several electrical wires from the arm; only three multipolar cables depart from the base to the outside, making the prototype portable.

The manipulation arms are also equipped with a sensory system which mainly counts on smart textiles. Electrolycra is a conductive textile which changes its electrical resistance when stretched and can be used in different configurations. Electrolycra based cylinders are placed along the arm and grouped in quadruplets (figure 3) to allow reconstruction of the arm pose (for further details see Cianchetti *et al* 2012). Furthermore, two parallel pieces of conductive material separated by a discontinuous non-conductive material are embedded in the arm skin. They are used to form the contact sensors that are capable of identifying forces high enough to put the two layers into contact (Hou *et al* 2012). The total length of the structure from the base to the tip is 300 mm, the diameter is 30 mm at the base and 14 mm at the tip.

The remaining six arms (R2 to R4 and L2 to L4), which are used for crawling, are based on silicone and cables. They embed a crank mechanism with features that allow octopus-inspired locomotion (Calisti *et al* 2012a). The locomotion arms are made of a silicone cone with a steel cable embedded axially. The arm is part of a three-bar mechanism, which replicates the four phases of the stereotypical pushing action of the octopus while crawling. This solution is based on a

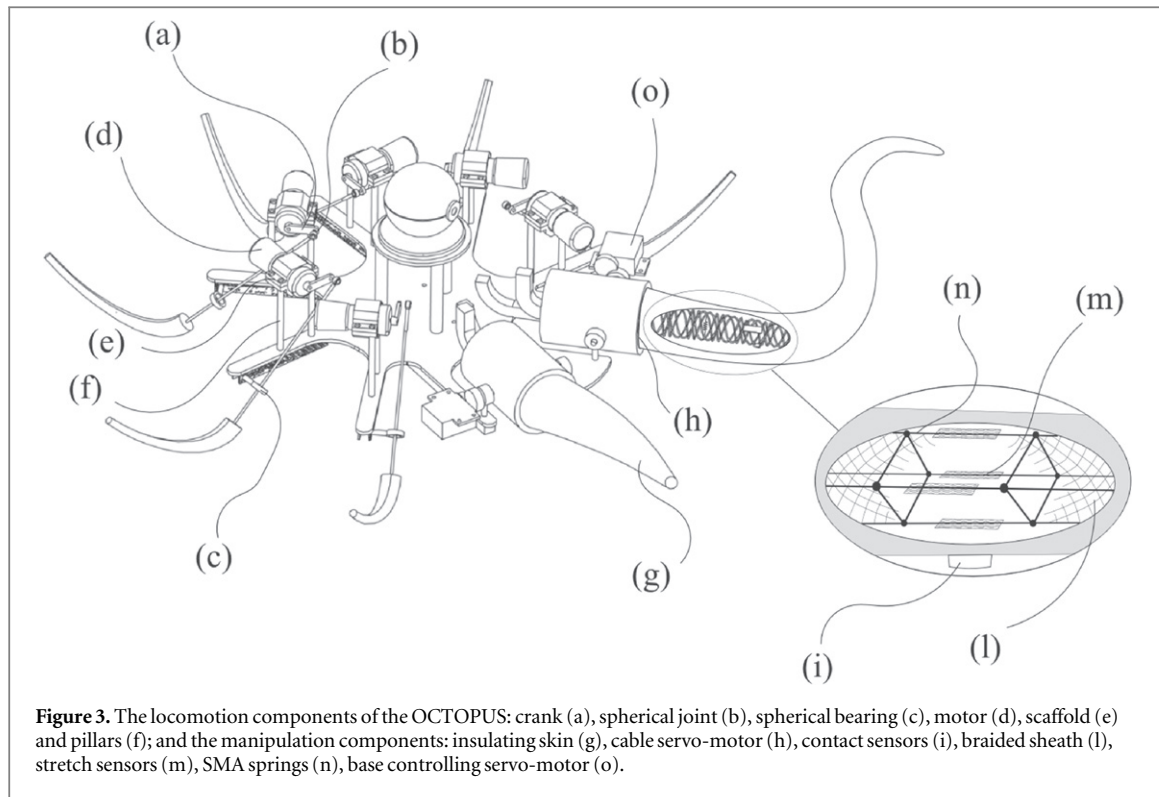


Figure 3. The locomotion components of the OCTOPUS: crank (a), spherical joint (b), spherical bearing (c), motor (d), scaffold (e) and pillars (f); and the manipulation components: insulating skin (g), cable servo-motor (h), contact sensors (i), braided sheath (l), stretch sensors (m), SMA springs (n), base controlling servo-motor (o).

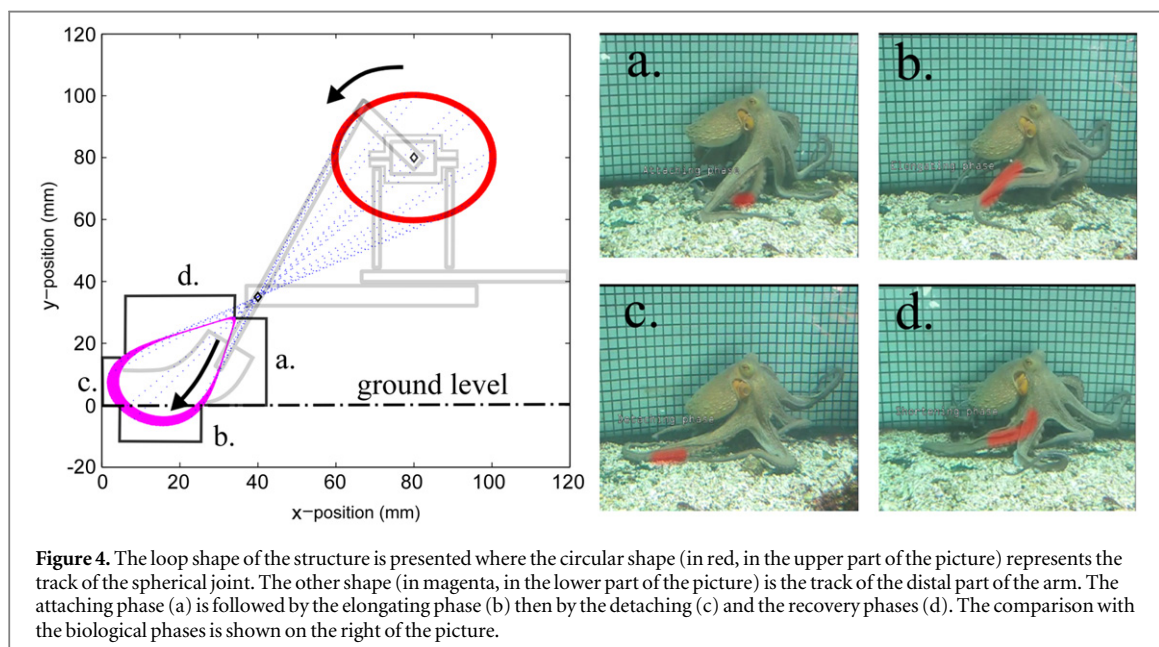
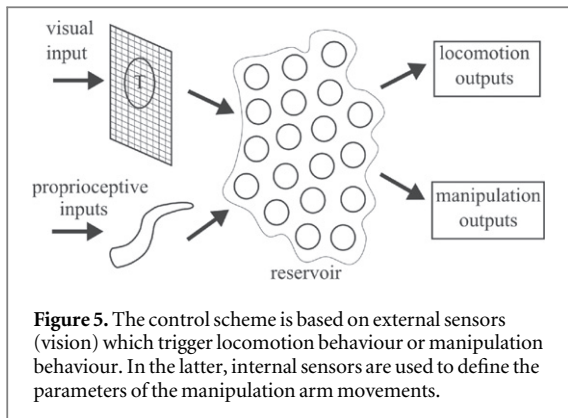


Figure 4. The loop shape of the structure is presented where the circular shape (in red, in the upper part of the picture) represents the track of the spherical joint. The other shape (in magenta, in the lower part of the picture) is the track of the distal part of the arm. The attaching phase (a) is followed by the elongating phase (b) then by the detaching (c) and the recovery phases (d). The comparison with the biological phases is shown on the right of the picture.

very abstract level with respect to the actual biological action: in living octopuses, the stereotyped movement of the arm is obtained with a sequence of actions that involve the coordination and contraction of several muscles. To achieve the first shortening phase, the proximal longitudinal muscles are contracted and the arm is moved towards the body. Then several suckers are attached to the substrate. The arm is capable of elongating, twisting, bending and shortening; this allows the sucker to be placed in the best position and to stick to the substrate. When the arm is firmly

attached to the ground, the radial muscles of the arm are contracted, thus elongating the arm and pushing the body forward. When the pushing phase ends, the suckers are released and the cycle can start again. The solution presented here only replicates the function of each phase. A parallelism between the biological action and the robotic action is presented in figure 4.

The design details of the mechanism can be found in (Calisti *et al* 2012a), nonetheless, the mechanism components are depicted in figure 3 and a brief description is reported here for the reader's



convenience. The crank is actuated by a dc motor, a rotational joint connects the crank to the steel cable of the arm and a spherical bearing (acting as a roto-translational joint) constrains the arm. It is worth noticing that the steel cables act as springs under the weight of the robot, representing a compliant interface between the robot and the environment. The motor is held in place by two small cylindrical pillars and by an insulating scaffold, which are lodged over an aluminium U-rod. Each mechanism is then radially lodged over the central base. The kinematics of the mechanism is shown in figure 4: the circular motion of the crank determines a specific loop where the four phases of the stereotypical pushing actions of octopus crawling are highlighted.

The locomotion strategy of the robot is based on a series of arms, called propulsive arms, which push/pull the body forward while the other arms, called stabilizing arms, keep the robot at a certain height from the ground. Even if the robot potentially performs several locomotion strategies (Arienti *et al* 2013), only two will be presented here. The first one is a pure pushing strategy, similar to the crawling strategy adopted by the octopus, where the robot simply pushes with the arms that are opposite to the desired direction. The second one employs both pushing and pulling actions. In this latter locomotion strategy, the propulsive arms are rotated to achieve a push or a pull, if the arm is opposite to the locomotion direction (rear arm) or is in the locomotion direction (frontal arm), respectively. In both strategies, the arms are activated in feed-forward control.

Both these locomotion techniques exploit the radial symmetry of the robot in order to obtain omnidirectional locomotion. By selecting a different set of arms, the robot moves in a different direction. This locomotion strategy is effective even if some of the stabilizing arms are busy or broken. Lastly, locomotion does not depend on the maximum number of arms of the robot, which is effective even if the arms are more than eight.

A float was lodged over the central base to enforce the desired density ratio between salt water and the OCTOPUS body. It is clear that a density similar to the

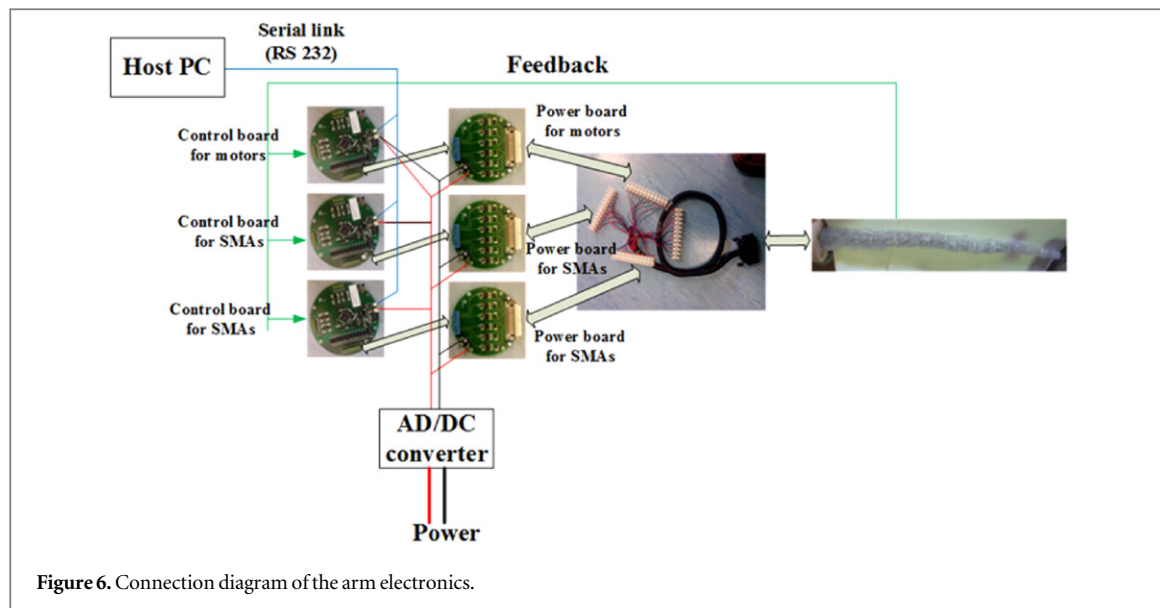
density of water helps the robot move with less force: this characteristic seems to be essential for the octopus' movements and indeed is replicated in the robot presented here. The robot density was designed to obtain a ratio between the density of the fresh water ρ_{f_water} and the density of the robot ρ_{robot} , $\rho_{f_water}/\rho_{robot} = 0.979$, which is the same ratio of the density of the salt water over the density of the octopus arms.

2.2. Control architecture

Despite the present work focuses primarily on the mechanical performances of the OCTOPUS robot, a brief excursus is reported below on the control architecture for the sake of completeness and for the reader's convenience.

The control scheme mainly consists of three components: a visual programme, a central control (reservoir computing) and a peripheral control. This scheme can be applied to both manipulation and locomotion. The central control receives sensory inputs from visual sensors and proprioceptive sensors, figure 5, and sends appropriate parameters for the desired behaviour to the peripheral control as outputs. Specifically, the imaging algorithm thresholds the image by using the colour of the target and consequently the centre of the target is extracted. The position of the target with respect to the robot is obtained from the position of the target in the frame. Regarding locomotion, the system takes visual information from the camera and sends out the direction of movement and its speed (rotation speed of the motor) to the locomotion arms, with the aim of approaching the target object (Li *et al* 2012). In this case the peripheral control simply drives the motor in clockwise or anti-clockwise direction, and the appropriate kinematics of the arm is ensured by the bioinspired mechanism.

Regarding manipulation, it takes visual information for locating the target and uses proprioceptive inputs from the SMA current sensors (providing the SMA activation state) to send out the parameters for the predefined basic motions to the manipulation arms. Reservoir computing (Schrauwen *et al* 2007) is a novel approach to build and train the recurrent neural networks. In this approach, only the connection weights from the reservoir to the output nodes are trained; thanks to this, many fast linear regression algorithms can be used. In our case, a reservoir computing approach is used to establish these sensorimotor couplings, and according to the target behaviour, the linear readouts are trained. Supervised training was applied: the target was placed in several places of the working space, and the robot was trained to associate the sensory-motor coupling (see Li *et al* 2012 for details). The peripheral programmes are located on each arm and use central commands to form time based commands for individual actuators in the arm. The peripheral control induces activation of the time-based selective actuators on the basis of



predefined sequences. As an example, the central control defines the orientation of the base of the arm and whether the arms should elongate or bend. Consequently, the peripheral control activates the specific SMA springs or cables with the proper timing.

The main hardware developed for peripheral control includes the control and power boards and the connecting cables. The control boards send the PWM signals to the power boards by using 24-pin connectors, the power boards are connected to the arm prototype through a 50-pin communication cable. Each control board includes 12-PWM outputs and a 16-channel A/D converter which are used to control the dc motors and SMA springs. The hardware system is shown in figure 6.

3. Experimental methodology

The objectives of the trials are to obtain data for common robotic tasks, such as locomotion and manipulation tasks. Furthermore, specific tests which highlight the peculiar capabilities of this soft robot were performed. Even if the comparison between biological and robotics experiments was arduous due to the complexity of both the animal and the robot, when possible, the data obtained from the robotic trials were compared with biological experiments.

3.1. Experimental tasks

A list of tasks was defined in order to demonstrate the capabilities of the OCTOPUS robot. Manipulation tasks aimed at evaluating the robotic performance of the manipulation arms in terms of working space, generated force, and exteroceptive and proprioceptive sensory performance. They are related to traditional tasks performed by robotic manipulators, such as the grasping of objects of different size and shape, the of

the manipulator, plus additional tests to validate the specific capabilities of the OCTOPUS prototype.

Regarding locomotion, they were mainly related to the octopus' crawling locomotion. The tasks related to locomotion focused on demonstrating how the robot can reproduce the crawling motion in different substrates with varying inclination, different combinations of arms and in the presence of obstacles. Specifically, three different substrates were used which represent three limit conditions: a smooth ground, a typical rough ground used in locomotion analysis and finally a ground with significantly high asperities, which was labelled as uneven ground. Details are presented in the next section. The rough ground was further employed to test the robot while moving on the inclined ground, with two inclinations of 10% and 20%. For each terrain, different activation strategies were also used, i.e. by using more arms for pushing and pulling. Finally, qualitative experiments on confined space were performed to highlight the peculiar passive capabilities of the soft robot.

Due to the nature of some of the manipulation and locomotion tasks, the control architecture of the robot was temporally disabled and the robot was activated manually to test each specific task. However, a complete autonomous task was performed to evaluate integration between the locomotion and manipulation behaviours, which included autonomous detection of a target, locomotion of the robot towards it, and grasping of the target to recover it.

3.2. Measured parameters

In order to assess the robot performances and allow objective evaluation and comparison, the tasks identified and listed above were quantified using broadly used parameters.

To quantitatively describe the performances of the manipulation arms, the maximum bending angles and

the definition of the working space were derived. Moreover, isometric force tests were performed to measure the force exerted axially by the arm and recorded with a dynamometer. Finally, contact sensor activation and the reconstruction capability of the stretch sensors were evaluated during grasping and other movements. Regarding contact sensors, specific tests were implemented to assess successful contact identification with the to-be-grasped objects. The curling effect implemented by the cable activation was then exploited to performing a grasping task for different shapes, i.e. four different objects:

- Object 1: rectangular cross-section wooden bar, 25 × 30 mm, 75 g weight.
- Object 2: round polymeric cylinder, 25 mm outer diameter, 58 g weight.
- Object 3: round polymeric cylinder tube, 60 mm outer diameter, 250 g weight.
- Object 4: round aluminium tube, outer diameter 25 mm, 478 g weight.

The functionality of the contact sensors embedded in the arm skin was tested in terms of missed detections. The aforementioned objects were located sequentially close to a contact sensor and a grasping task was initiated. During this operation, the contact sensor was expected to detect obstacle collision while the arm was already starting to wrap itself around the object. Missed detections were recorded and used to calculate the hit ratio of each single contact sensor during the grasping operation.

Two main parameters were taken into account for crawling locomotion: the speed of the robot and the cost of transport (CoT). The speed was evaluated as the space covered during a trial over the time required to finish the trial. During crawling, speed is not constant, so a mean speed was evaluated and used to easily compare different trials; locomotion dynamics was also recorded to analyse specific conditions. The CoT is becoming a common parameter to evaluate robot locomotion. It calculates how much energy is required by a robot to move and is used to compare objectively different robots. It is presented in different equivalent forms, and here the following is used:

$$\text{CoT} = \frac{W}{v \cdot P},$$

where W is the power absorbed $W=V \cdot i$, with V voltage applied, i , current absorbed during the trials, P weight of the robot and v mean speed of the robot. Additional parameters were derived, such as step amplitude, elongation of the arms, ratio between arm elongation and step amplitude and direction of locomotion with respect to arm elongation. This elongation is derived from the mechanism already described in Calisti *et al* (2012a), where the kinematics is defined by the geometrical parameters of the mechanism, such as the length of the crank, the distance between the centre of rotation of the motor

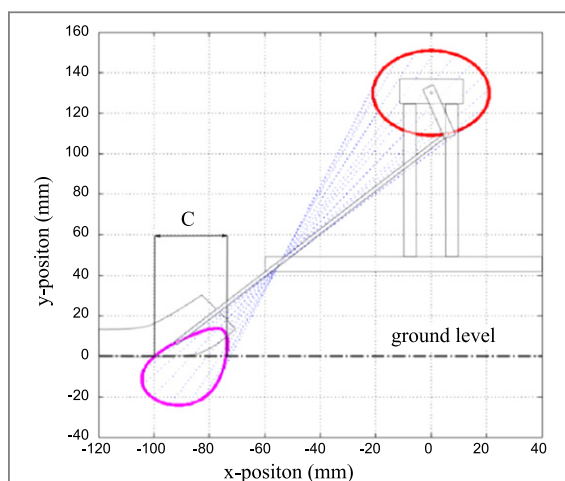


Figure 7. Locomotion mechanism and the loop of the distal part of the arm. As in the octopus, the elongation of the arm causes a translation of the robot body forward while it is in contact with the ground.

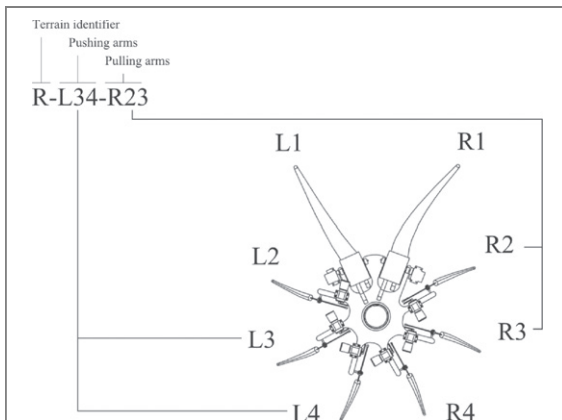


Figure 8. Trial labelling. This trial identifier example shows crawling on rough terrain with arms L3 and L4 pushing and arms R2 and R3 pulling.

and the spherical bearing and the length of the arm (see figure 3).

In figure 7, the part of the loop that is in contact with the ground while the arm is pushing is highlighted and labelled as C and this is considered to be the maximum distance achievable at each push. The ratio between the actual step length of the robot (s_l) and the maximum distance achievable define the effectiveness of the step r_e . In the real octopus, the elongation of the arm has exactly the same value as body translation, thus $r_e = 1$.

3.3. Experimental setup

The measurement of the parameters reported and described in the previous section required specific setups.

3.3.1. Trial identification

Each trial in the text will be identified by an alphanumeric code such as: R-L34-R23. The first letter

Table 1. Surface features.

ID	Description	Spike height (mm)	Spike distance (mm)
S	Smooth ground	<0.01	<0.01
R	Rough ground	~0.1	~0.5
U	Uneven ground	~10	~20

identifies the ground, where S stands for smooth ground, R for rough ground and U for uneven ground. The first set of numbers, until the dash, identifies which arm is pushing. The second set identifies which arm is pulling. An example is presented in figure 8.

3.3.2. Pool and terrains

The main experimental setup was composed of a swimming pool, where the robot moved, grasped objects and squeezed between obstacles. An external recording system, based on two cameras, was used to retrieve the three-dimensional positions and the orientation of the robot. The swimming pool was a steel frame pool measuring 260 cm × 170 cm × 61 cm which was filled with 20 cm of fresh water ensuring complete submersion of the robot, except for the camera. Various substrates were placed on the bottom of the pool in order to test the locomotion capability of the OCTOPUS robot. They featured different spike heights and distances, as illustrated in table 1. They can be classified as smooth ground (polished ground without asperities), rough ground (ground with small asperities) and uneven terrain (terrain with regular spikes of about 10 mm). It is worth remembering that the diameter of the supporting base of the locomotion arms has a diameter of 25 mm, thus in the case of the uneven terrain, the height of the spikes and the distance among them were respectively 40% and 80% of the arm size, representing, therefore, a truly uneven terrain for the robot.

The R-surface was also used to prepare an inclined terrain. Small blocks were assembled to obtain two different slopes with 10% and 20% inclination. The R, U and the inclined block are shown in figure 9. In each locomotion trial the robot moved from one side of the swimming pool to the opposite one, or from the lower to the upper side of the inclined ground.

Table 2 reports the trials performed to evaluate the OCTOPUS locomotion. Y cells mean that the results of this specific trial were reported, N cells mean they were not. It is worth mentioning that all the combinations in table 2 were tested, however only the results of the successful tests are reported.

All arm combinations were reported for R-S-U grounds. For the specific case of inclined grounds, it appeared that the robot was able to climb the slope only using four arms, for example in the R23-L23 combination.

3.3.3. Recording system

The robot moved over a planar surface inside a working space of about 260 cm × 170 cm × 20 cm and

eight markers were placed on the vertexes of the working space. The markers which define the working space were used to calibrate two high speed cameras to perform direct linear transformation (DLT). This transformation allows reconstruction of a 3D scene from two or more bi-dimensional images. We used the least square method in these trials to derive 11 DLT parameters for each camera: $C_{i,j}$ with $i = 1, 2$ and $j = 1, \dots, 11$. The eight working space markers were used as control points to derive the DLT parameters: it is worth noticing that the minimum number of control points required to derive 11 DLT parameters is six. However, since all the vertexes of the control space were available, eight control points were used, which resulted in increased reconstruction accuracy (Chen *et al* 1994). Other three markers were placed onto the robot, see figure 10. The position of the centre of the robot and the orientation of the body were retrieved by the three markers on the central platform; this was possible when the three points did not belong to a line. After calibration, the three-dimensional positions of the three robot markers were reconstructed and the centre of mass of the robot was derived. To extract the parameters of the different trials of the robot, the state of the robot was defined as the x, y, z positions of the centre of mass as well as its orientation with respect to the yaw, pitch and roll angles.

The working space of the manipulation arms and the reconstruction of its pose were evaluated using a similar technique despite using a simpler recording system.

3.3.4. Isometric force measures

An effective set-up already used to evaluate the isometric forces generated by the octopus arm is the most suitable instrument to assess the OCTOPUS capabilities. Details on the instruments are reported in Margheri *et al* (2012), but their main features are recalled here for the sake of completeness.

In its simplest configuration, the instrument consists of a graduated tube of transparent Plexiglas joined to a support plate with dimensions depending on the size of the animal. To measure force and stiffness, a load cell was integrated in the setup. The apparatus is intended to measure one arm at a time (as shown in figure 11 with the support plate keeping the octopus body apart) and is adapted for this purpose using sensors (i.e. load cells) and mechanical components (i.e. springs). The cylindrical base of the arm was fastened in a fixed position in the testing tank. The set-up was mounted and blocked on the side of the tank and the tip of the arm was mechanically secured to an inelastic cable connected to the digital dynamometer.

4. Experimental results

The numerical performances extracted from the OCTOPUS robot are reported in this section.

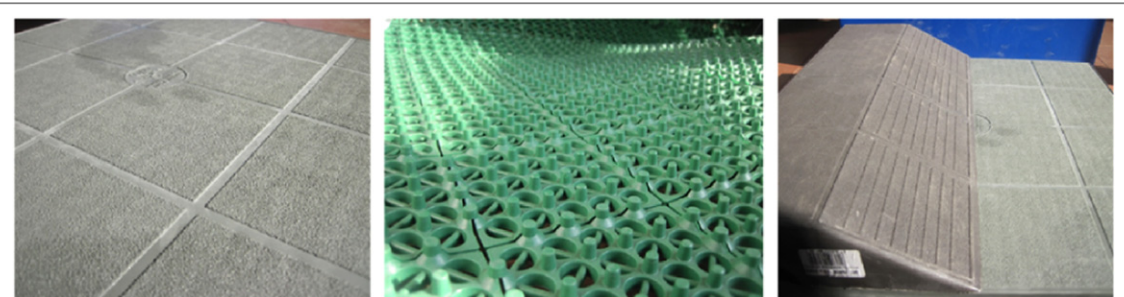


Figure 9. From left to right: rough terrain (R), uneven terrain (U) and inclined block.

Table 2. Trials presented by kind of ground and arms used.

Arm(s)	R	R-Slope1	R-Slope2	U	S
R4; L4	Y	N	N	Y	Y
R4L4; R34; L34	Y	N	N	Y	Y
R34L4; L23R4	Y	N	N	Y	Y
L3-R2; R3-L2	Y	N	N	Y	Y
R23-L23	Y	Y	Y	Y	Y

4.1. Manipulation working space and force measurements

The manipulation working space was evaluated by measuring the limit angles achievable by the arms. The robot was located in a fixed position in the centre of the testing pool. Arm motion during different actuation sequences and modes (using both cables and SMA springs) were recorded and processed using the setup mentioned in section 3.3.3. The combined use of the longitudinal cable and the local SMA springs introduced a rich variety of movements defined in a 3D workspace. It is worth mentioning that the angles of operations reported here do not represent the maximum capabilities of the SMA springs since a precautionary power limitation was imposed to preserve the functionality and life of the actuators.

The chosen number and arrangement of the SMA actuators defined whether to bend the manipulation arms in three different points along the arm (figure 12), but with different angles. Values referring to the mean of five trials are (from the base to the tip) $\alpha = 76$, $\beta = 44$ and $\gamma = 57$ deg of bending angles.

It is worth underlining that the reported angles represent the maximum angle achievable when they are activated all together at the same time. When singularly activated they are all able to reach higher values. When only α and β are activated (for example) they achieve 78 and 55 deg respectively and if only α is used the angle reaches the highest value of 85 deg.

These results show that the SMA springs reach a lower limit angle if coupled with the activation of other springs. The most reasonable hypothesis which justifies this behaviour can be found in the internal mechanical state of the arm itself during motion. Spring activation deforms the braided supporting structure of the arm and due to its nature it propagates deformation longitudinally and radially. The

activation of the actuating elements increases the internal stress state of the arm so that the greater the number of springs used, the lower the deformation they are singularly able to produce.

While the SMA springs have a local effect, activation of the longitudinal cable determines the curling of the entire arm on itself. In order to describe the free motion working space of the manipulation arms, the two effects have to be summed. The working space is thus the union of the working areas defined by the activation of SMAs on the horizontal plane and the cable on the vertical one. Experimentally extracted, the working space volume is defined horizontally by an area of 400×440 mm with the qualitative shape shown in figure 13(a), while on the vertical plane the arm moves in a 290×150 mm space within the qualitative shape shown in figure 13(b).

The forces generated by the soft manipulation arms were evaluated using the set-up mentioned in section 3.3.4, purposely realized to measure the forces which are exerted by its biological counterpart (the real octopus arm).

The dynamometer included in the set-up revealed the following peaks of axial isometric forces: 1.2 N by activating the longitudinal SMA springs and 10.8 N by pulling the longitudinal cables. As expected, the force produced using the cable is much higher than the results achieved by the springs, confirming that with a combination of small SMA springs and a motor-driven cable the arm is able to cover a wide spectrum of applications: the former for local activation (to provide high mobility), the latter for global motions and powerful actions (despite the servomotor bulkiness). Actually, SMAs are well known for their very high force density, but in order to obtain the necessary performance in terms of stroke within the available space and without achieving prohibitive values in terms of power consumption, a helicoidally shaped (springs) resulting in a trade-off with the produced force.

4.2. Sensor evaluation

Contact sensor activation was evaluated averaging the results obtained on 20 trials carried out for each object on each sensor. Results are reported in table 3.

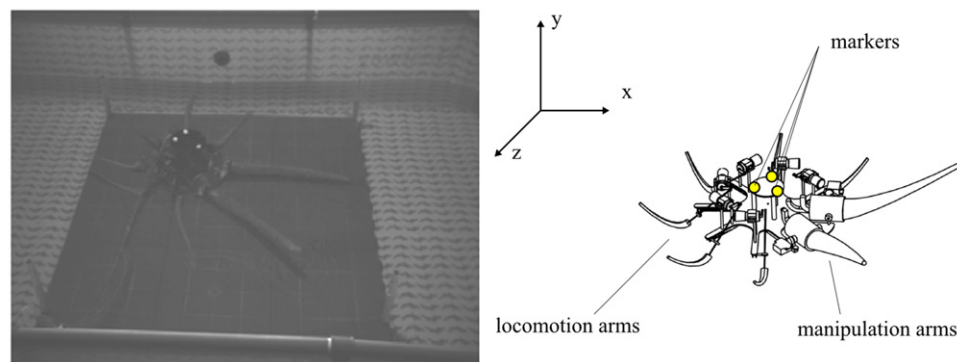


Figure 10. Example of working space and positioning of markers.

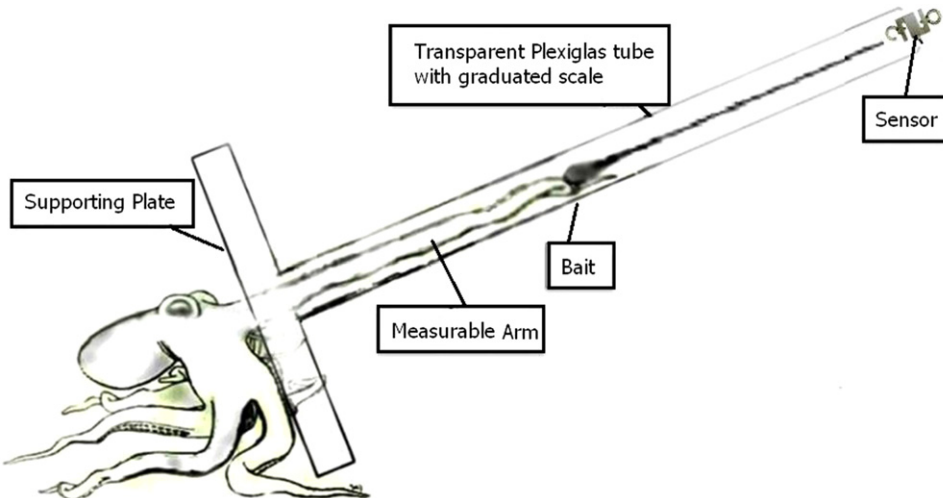


Figure 11. Drawing of the force measurement set-up, here approached by a real octopus pulling the cable connected to the force sensor.

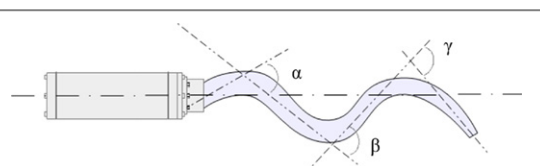


Figure 12. Bending motion capabilities driven by SMA actuators: α , β and γ represent the three achievable angles.

To estimate the manipulation arm pose, the angles created in the robot during operation were measured (figure 15). Thirty different arm poses were derived using image reconstruction techniques and the angles for each of the five virtual segments into which the arm is divided (due to the discretization induced by the local stretch sensor quadruplets) were evaluated. Signals from the stretch quadruplets were converted into bending angles and saved in a file representing each pose as described in Cianchetti *et al* (2012). Tabular data from both photogrammetry and shape-reconstruction computed angles were used to evaluate the reconstruction error in terms of angle difference, as shown in table 4.

Mean angular error among all quadruplets is about six degrees. This is an acceptable error compared to the benefit derived from using a series of novel soft sensors purposely developed to be mechanically resilient and down scalable and to work under high deformation conditions.

4.3. Crawling speed and CoT

This section reports the results on the crawling speed and the CoT. The tracks in figure 16 illustrate how the centre of mass of the robot moves with respect to the reference frame. Even if the robot started from different positions in each trial, all tracks were reported to the origin after reconstruction to ease comparison among them. For this reason the y -track also has negative values.

Speed and CoT results were grouped for kind of substrate and for number of arms involved in the locomotion. As an example, from the S-L34R4 trial reported in figure 16 it is possible to derive directly the mean speed v by the x -track, that is about 1.9 cm s^{-1} . The mean value of each group is reported in figure 17(a) while the error bars indicate the standard deviation. It

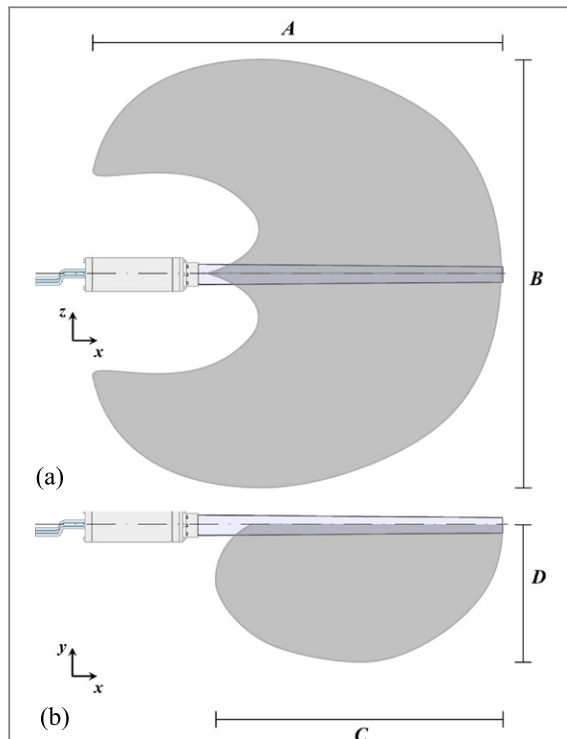


Figure 13. Working space dimensions: in the horizontal plane $A = 400$ mm and $B = 440$ mm (a); in the vertical plane $C = 290$ mm and $D = 150$ mm (b).

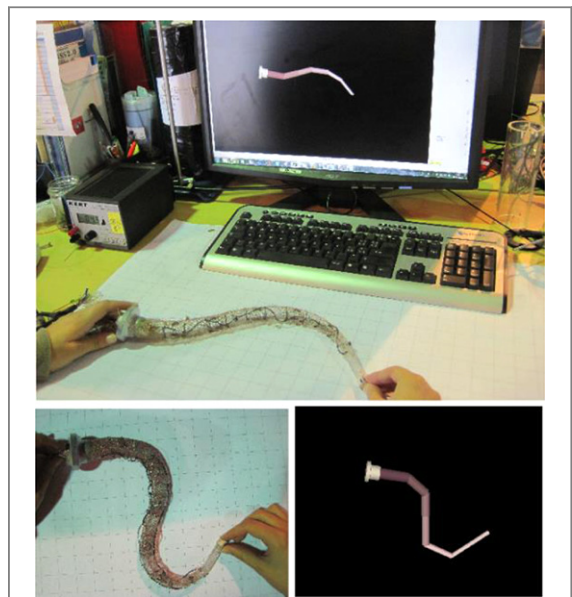


Figure 15. Measurement of error in pose reconstruction: comparison between the real shape and its 3D visualization after processing the stretch signals from quadruplets.

Table 4. Errors on the estimation of angles for pose reconstruction.

Virtual segment number	Angle error mean (deg)	Angle error max (deg)	Angle error min (deg)
1	5.67	14	2
2	7.44	24	1
3	6.11	14	0
4	5.78	27	1
5	6.67	29	0



Figure 14. The OCTOPUS robot while performing axial isometric force measurement.

Table 3. Sensors activation (hit ratio) while grasping different objects.

Sensor no.	Object 1	Object 2	Object 3	Object 4
1	13/20	17/20	18/20	17/20
2	17/20	18/20	19/20	20/20
3	18/20	18/20	20/20	20/20
4	17/20	20/20	20/20	20/20
5	13/20	17/20	17/20	18/20

shows that the crawling speed is almost constant with respect to the tested grounds. Conversely, when the speed is evaluated with respect to different actuations, a difference in performance was found: by using more than one arm to push, the speed of the robot almost

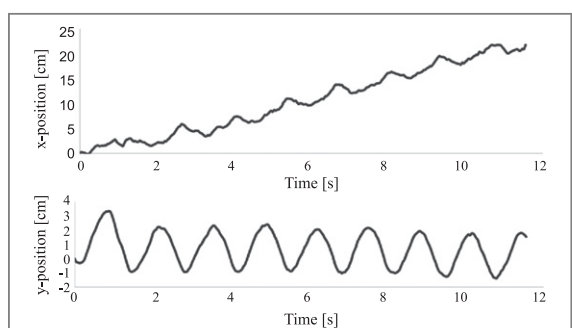


Figure 16. The *x* and *y* tracks of trial S-L34R4. The *x* represents the motion along the horizontal axis (top), while the *y* identifies the oscillations on the vertical axis (bottom). The track on the *z* axis is not reported, since it was almost constant during this trial.

doubles (figure 17(b)). As a further benefit in using more arms, it is worth remembering that the robot was not able to climb the slopes using one arm, so this suggests that the coordinated use of four arms can prompt the best performance in the OCTOPUS prototype. Moreover, even if not reported in the statistical analysis, it is worth noting that a speed of up to 5 cm s^{-1} was achieved in a few trials, when a sort of arm coordination emerged during feed-forward control.

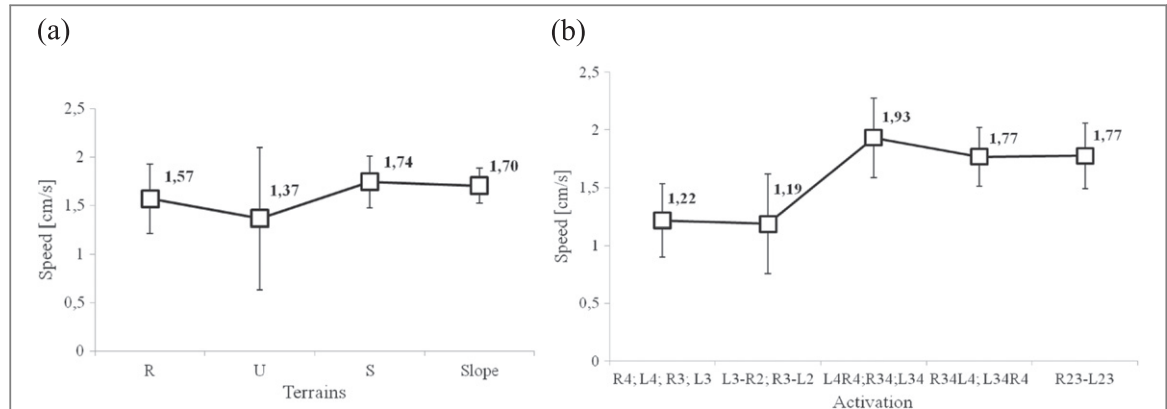


Figure 17. Crawling speed with respect to several ground (a) (data about slope1 and slope2 are merged together) and to different activations (b).

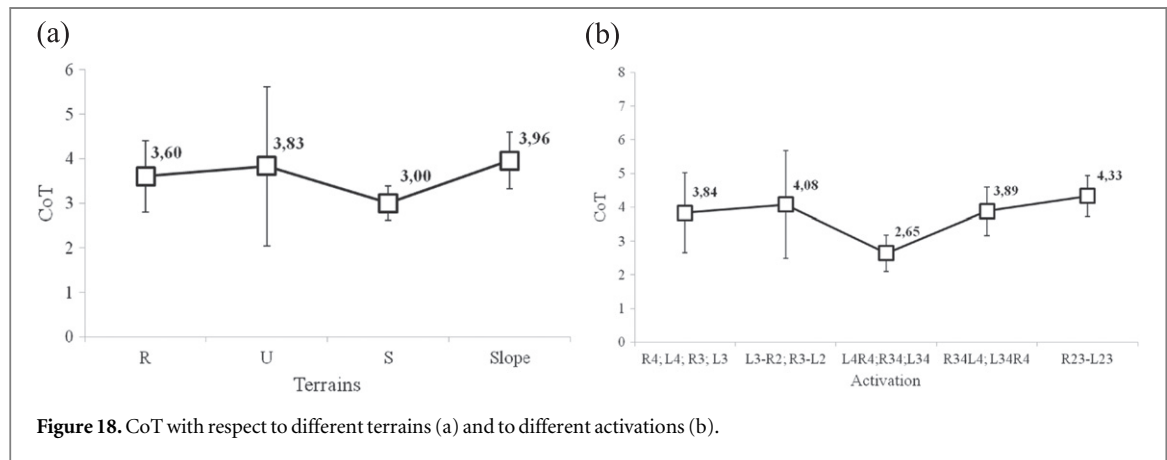


Figure 18. CoT with respect to different terrains (a) and to different activations (b).

The CoT is derived by considering that $V=5$ V, $i=0.32$ A and the weight of the robot is $P=3 \cdot 9.81 = 29.43$ N. With these data, referring to the example reported in figure 16, the CoT becomes:

$$CoT = \frac{5 \cdot 0.32 \cdot 100}{1.9 \cdot 29.43} \cong 2.9$$

As for speed, the CoT is calculated and reported with respect to different activations and terrains (figure 18). It is possible to state that it changes slightly with respect to different terrains: the results do not show significant correlation between the terrain type and the CoT, which ranges from 7 to 1.8 (figure 18(a)). Although speed is higher when more arms are used (figure 18(b)), if we consider the CoT with respect to arm activation, a minimum value appears when two arms are activated in pushing condition.

Finally, the additional parameters derived are the mean step length and the ratio between step length and arm elongation. The step length was evaluated from the tracks in figure 16. The y -track was used to derive the start and end of each step: one step is considered to start at the apex of the y -track (that means y is locally maximum and y speed is null) and is considered to end at the next apex. Eight steps were considered in the trial reported. The length of each step was estimated by subtracting the x position at the end and at the

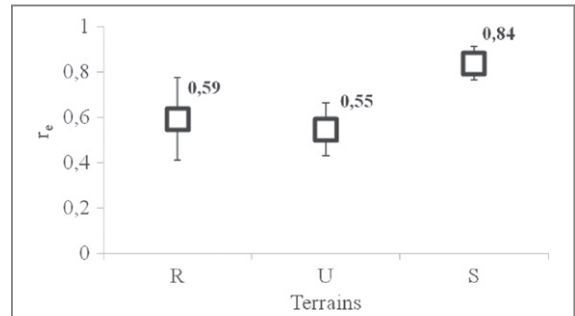


Figure 19. Step effectiveness over different grounds (slopes are not reported, since the steps were too difficult to evaluate). The smooth terrain represents the terrain where OCTOPUS has the highest step effectiveness.

beginning of each step: the mean length was then directly derived and was $s_l = 2.8$ cm.

By recalling the crank mechanism reported in figure 3 and the overall dimensions of the robot, the current value of C is about 3 cm, thus the ratio for the S-L34R4 trial is:

$$r_e = \frac{s_l}{C} \cong 0.93$$

The mean values of step effectiveness are reported in figure 19 together with the corresponding standard

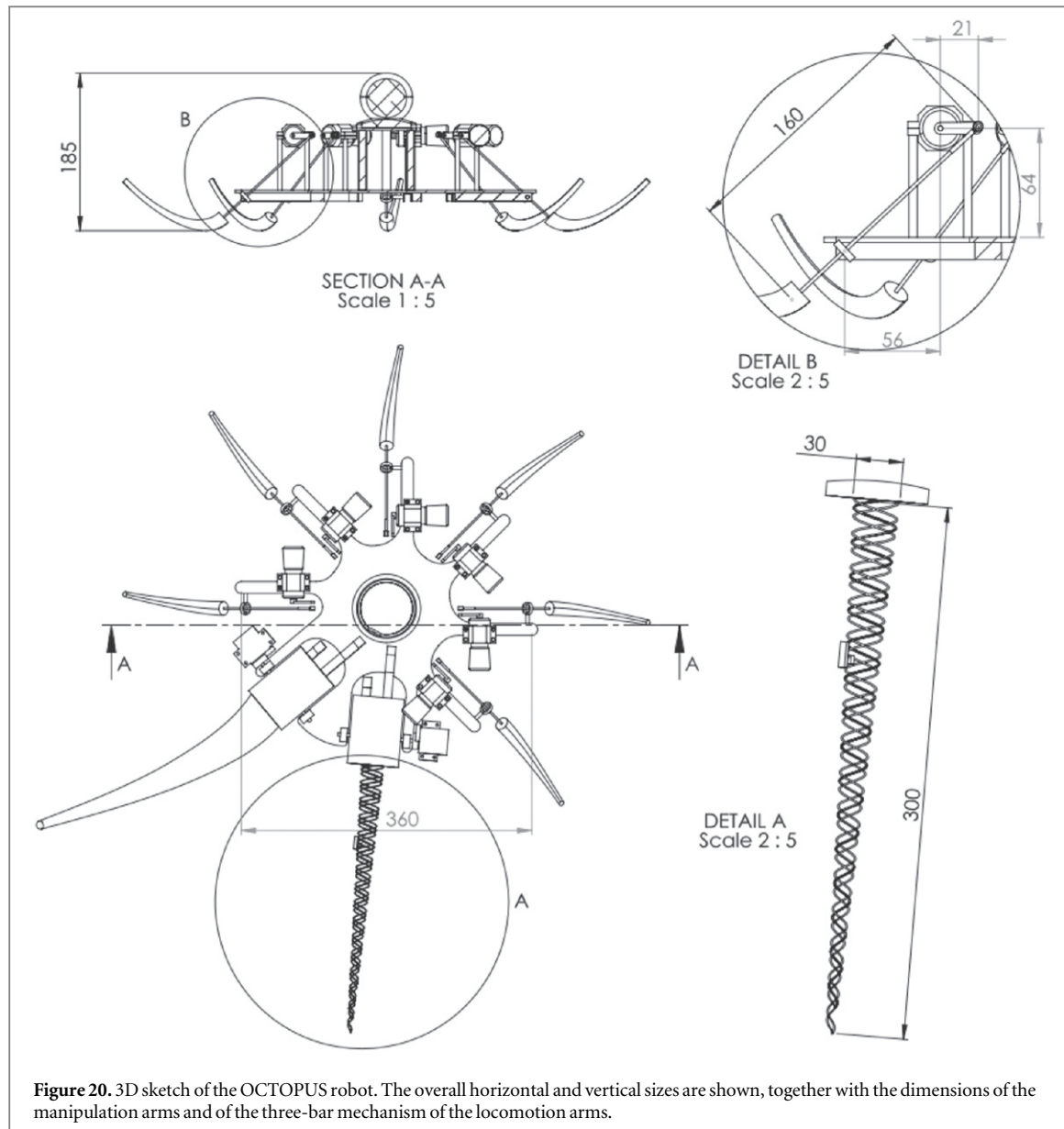


Figure 20. 3D sketch of the OCTOPUS robot. The overall horizontal and vertical sizes are shown, together with the dimensions of the manipulation arms and of the three-bar mechanism of the locomotion arms.

deviation. The maximum value was obtained for smooth ground and was $r_e = 0.96$.

4.4. Specific trials

This section reports the locomotion results regarding two particular manoeuvrability tests: the capability to move through passages narrower than the robot's nominal diameter (from one tip to the tip of the opposite arm) and the capability to cope with discontinuous terrains. Finally an autonomous object recovery task was implemented to test the synergetic coupling of omnidirectional locomotion and adaptable grasping.

The robot was made to pass between two fixed obstacles (i.e. two jars) which were at a distance requiring considerable deformation of the OCTOPUS platform. The diameter of the robot was about $D = 1$ m, while the distance between the two jars was about $d = 0.4$ m (the diameter of the rigid central body of the robot was about 0.36 m), see figure 20. Even if it does

not present quantitative data, this peculiar test highlights the soft properties of the robot. Locomotion in confined spaces is a challenging task for traditional hard robots, however this preliminary test demonstrates that a soft robot is able to cope with this kind of hostile environment passively.

One of the advantages of legged robots with respect to wheeled locomotion is that they are able to pass over gaps in the ground. This test was performed by separating two of the ground blocks used during the trials. The gap width is about 5 cm, which is greater than the elongation movement of the arm. As for the passage between obstacles, here the robot arms were manually controlled. An example of successful crossing of the gap is presented in figure 22.

Finally, qualitative results are reported for the autonomous object recovery test introduced at the end of section 3.1. Training was performed in a manner similar to (Li *et al* 2012) with small differences: since the locomotion arms were located on the rear part of the OCTOPUS, locomotion was not omni-

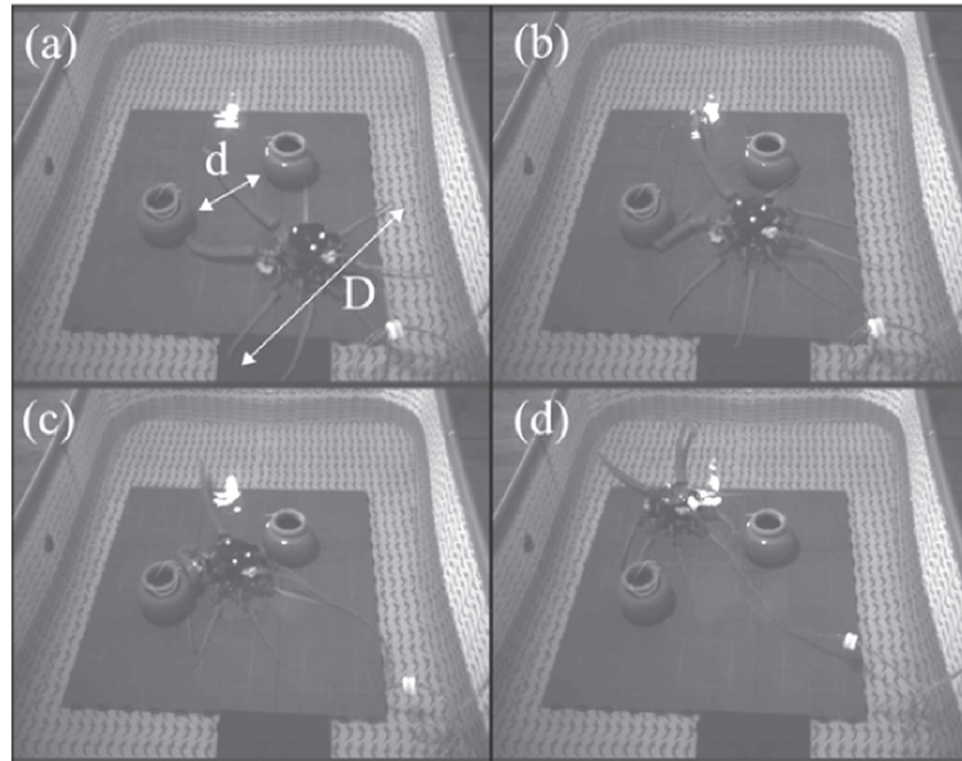


Figure 21. Snapshots of a trial regarding the passage between obstacles. Figure (a) depicts the starting position of the robot, together with the distances tip to tip of the arm and jar to jar. In figure (b), the robot is approaching the passage and a manipulation arm is squeezed to the body. In figure (c), the robot is between the two jars: one manipulation arm is completely curled towards the body, while two locomotion arms are inclined backwards. In figure (d) the robot has successfully passed the obstacles.

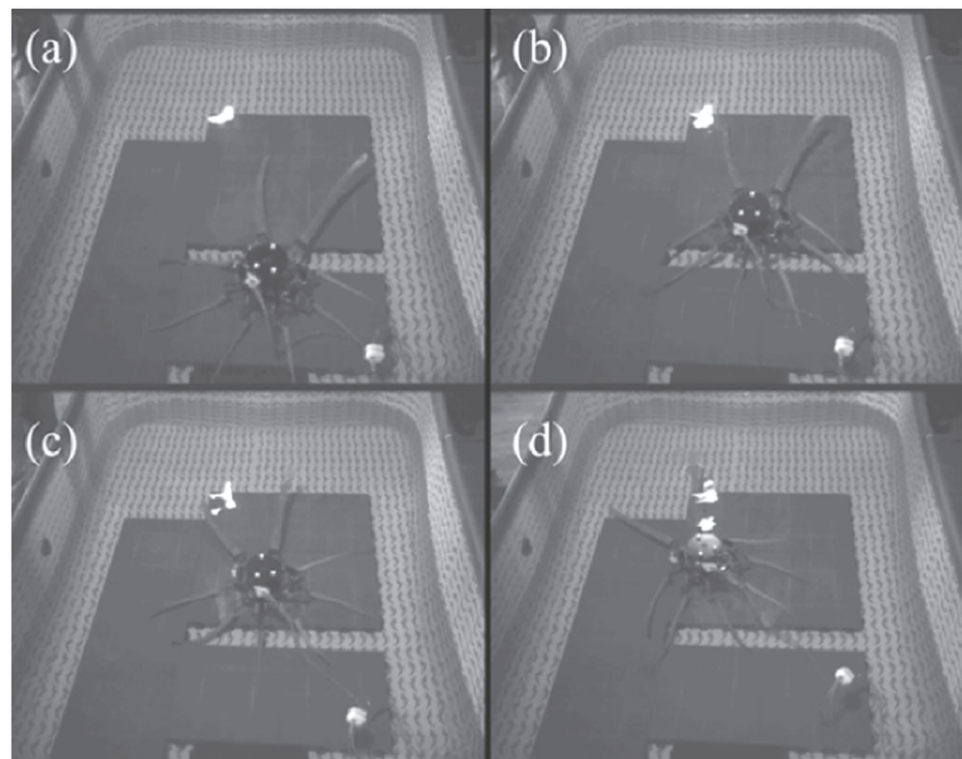


Figure 22. The gap crossing: the gap is initially approached (a); half of the body has passed over the gap (b): the rear arms can no longer effectively push the robot, so the frontal arms are used (c); finally the gap is successfully crossed (d).

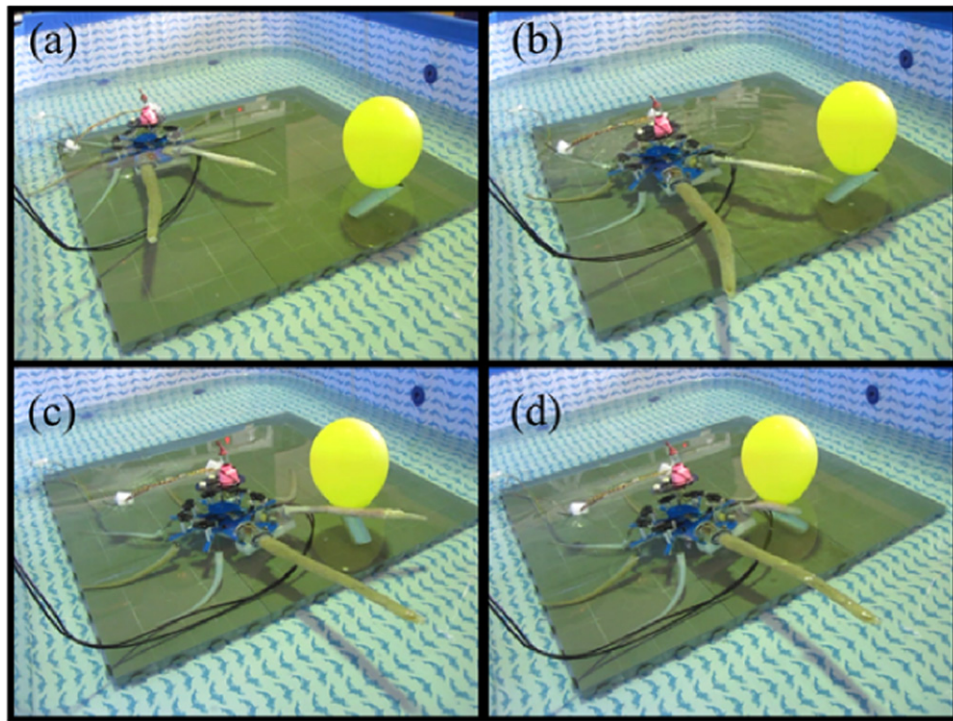


Figure 23. Phases of the behavioural task: the submerged robot detects a target and activates the correct arms at high speed (a) and then at low speed (b). When it is close enough to the target (c), the manipulation arm is activated to grasp the object (d).

directional. The robot was trained to move forwards, to the right or to the left. Even if it is possible to change the robot's orientation with specific actuation strategies and timing, this movement was not trained. The four phases of the behavioural task are shown in figure 23.

The speed of the robot was varied by reducing the pushing frequency and the grasping action was obtained via activation of the longitudinal cable.

5. Discussion

OCTOPUS is currently one of the first soft robots which is effectively provided with both locomotion and manipulation capabilities. It implements several features discovered in the real octopus, i.e. a pushing-based locomotion mechanism, an arm structure based on morphological observation and control strategies which exploit the robot mechanics. A discussion on the performances of this robot is reported in this section, together with a comparison which highlights, quantitatively when possible and otherwise qualitatively, the biological features that were successfully translated into the robotic artefact.

5.1. Robotic performances

Motion and grasping have been reported and detailed and the results show that it is possible to obtain a three-dimensional complex workspace by combining the local (SMA springs) and the global (cable-driven) actuation systems. This is a quite unique characteristic

with respect to the bioinspired manipulation arms currently available in literature and reported in the introduction. With respect to these robots, OCTOPUS presents two main drawbacks: a lower payload and accuracy, but on the other side it shows intrinsically safe interaction, higher dexterity and adaptability together with the possibility to be used underwater. The OCTOPUS manipulation arms are able to handle different sized objects thanks to their shape and flexibility. The arms not only behave like underactuated structures, but, unlike a cylindrical arm, during bending the conical shape of the OCTOPUS braided sheath creates a non-constant curvature arc (actually a spiral-like shape) from the base to the tip which enhances its conformability to objects.

These peculiar manipulation abilities are combined with advanced locomotion capabilities.

A comparative quantitative analysis with other underwater robots implementing crawling locomotion is limited since there are only two other robots (up to the authors' knowledge) which have this capability: the Crabster and the robotic lobster.

Even if we extend the comparative analysis to the terrestrial environment, since underwater legged locomotion has several peculiar features (i.e. influence of the drag and lift force, role of density, role of buoyancy force with respect to the force of gravity, etc...) a direct mapping between terrestrial legged robots and the OCTOPUS prototype is not straightforward.

As reported in section 4.1, the speed of the OCTOPUS is independent from the ground analysed and reaches a top speed of 5 cm s^{-1} which corresponds to about 0.3 BL s^{-1} , and a minimum CoT of about 1.8.

Compared to the other underwater crawling robots, OCTOPUS is slower than the Crabster robot which reaches a speed of about 1 BL s^{-1} (where the length of the legs is considered as body length), but considerably advantageous with respect to the CoT value, which is about 10 for Crabster (Kim 2013).

The speed of OCTOPUS is lower than other traditional terrestrial legged robots, however it is among the highest for legged soft robots: as an example, the speed of the successful multi-gait soft robot presented in Shepherd *et al* (2011) is about 2.5 cm s^{-1} (corresponding to 0.053 BL s^{-1}). The CoT is in between common robot performances: the Cornel ranger, the ‘cheapest’ walking robot, has $\text{CoT} = 0.28$, while Asimov by Honda has $\text{CoT} = 2$ and BigDog by Boston Dynamics has $\text{CoT} = 15$ (Cotton *et al* 2012). With respect to activation, of interest is that the CoT does not increase with a growing number of activated arms. This depends on the ratio among power consumption W and speed v : data revealed that when three and four arms were activated, both W and v increased keeping their ratio constant while, on the other hand, when two pushing arms were activated the CoT related plot has a minimum. This could suggest that, even if pulling arms are required together with pushing arms for inclined grounds, the optimal trade-off between speed and power consumption can be obtained with two pushing arms. Finally, it is worth highlighting that when the highest speed is achieved, i.e. 5 cm s^{-1} , the CoT decreases to the lowest value of 1.8. However, the most peculiar performance of this soft robot is the passive ability to squeeze its arms in small apertures: as illustrated in section 4.4 the robot is able to locomote through spaces almost as narrow as its rigid central part thanks to the softness of its arms. But this feature also affects the carrying capabilities of the robot and, despite no quantitative data have been gathered yet, we can anticipate that this compliance limits the maximum transportable weight.

It is important to add that some performance limitations (in numerical terms) were introduced given our aim to obtain a complete and integrated robot with both manipulation and locomotion capabilities, but if studied separately and with a task driven approach they have already proved to achieve better performances (Laschi *et al* 2012).

5.2. Biological translation

Owing to the extreme hyper redundancy of its very flexible body, the octopus needs to adopt smart solutions to control itself. It has already been shown that for some of its single-arm movements one of the ways with which the octopus copes with this burden is by exploiting its body features. An in-depth analysis of the octopus arms revealed their shape and morphological features, translating them into design concepts for soft-robotic components.

The arm specialization observed in the real octopus was used to separate the locomotion and manipulation design approach and this allowed effective exploitation of the octopus-like features recreated in the OCTOPUS robot. In the manipulation arms, this enabled the replication of octopus-like movements with local control of the arm shape. Several tasks can be accomplished by the arm as a consequence of the combination of simultaneous activations of the single springs. In particular, it is possible to obtain elongation, shortening and local bending, which are the basic movements the octopus performs and combines to generate more complex actions.

Moreover, the complete absence of rigid parts makes it possible to replicate the high compliance and flexibility of the octopus arm but at the same time also the capability to generate relatively high forces when needed.

The bioinspired design of the sensory system allows a complete understanding of the status of the arm and of the proximal surrounding environment. These functionalities, now used for pose reconstruction and object grasping purposes, will enable the implementation of even more complex capabilities shown by the real octopus (i.e. shape and texture discrimination—Wells 1978).

Analogously to the functional translation of the arm features for reconstructing manipulation capabilities, we derived the fundamental functions of crawling based on pushing. The crawling locomotion of the OCTOPUS prototype shares and takes inspiration from several of these features. The fact that all the arms only push by elongation and contribute identical forces greatly simplifies control meaning that, each time, the octopus simply has to decide which arms it will use and not how to use them. We have shown that each of the arms that are involved in crawling also follow a predefined stereotypical motor programme (Levy and Hochner 2010). The rhythmical four phase pushing locomotion that has been found in octopus crawling was directly implemented in the robot. Moreover, the robot is able to move in every direction by pushing with different arms and by using a vector combination of the pushing actions. A feed-forward control was used to rotate the locomotion arms, and the three-bar kinematics implemented an effective pushing action of the distal part of the arms. The OCTOPUS successfully coped with crawling over different substrates and terrains, as performed also by the biological counterpart.

Moreover, by proper controlling the timing of the pushing/pulling action, OCTOPUS can also implement a coordination strategy enabling it to rotate its body on the spot. These particular strategies were implied in more complex locomotion tasks, such as squeezing between obstacles or overpassing terrain gaps. As last remark, the robot is slightly slower than the biological counterpart, i.e. OCTOPUS prototype achieves 5 cm s^{-1} (0.3 BL s^{-1}), while the speed of its

biological counterpart is about 7.3 cm s^{-1} (0.6 BL s^{-1}) (Huffman 2006). Finally, while the real octopus has a maximum effectiveness of step, the OCTOPUS almost reaches the same value (0.93), yet without employing any active attachment strategy.

As additional remark, it is important to notice that octopuses use tactile and proprioceptive sensors to interact with the environment. If a properly high number of sensors are added on the locomotion arms, it would be possible to automatize some behaviours (as for example navigation through realistic environments) without the visual input. In this sense, a preliminary investigation has been performed in Calisti *et al* (2012b) where current feedbacks have been implied in arms coordination. However, the control of soft robots through distributed sensors is a very difficult as well as very interesting topic which deserves a deep investigation and involves not trivial solutions, that were not treated in this paper to avoid loss of focus.

6. Conclusions

This paper presents the results of the experimental characterization of the OCTOPUS robot. The tests assessed the robot's performance with respect to traditional robotic tasks and to the biological counterpart. The OCTOPUS robot represents the first example of a soft underwater robot which is provided with manipulation and locomotion capabilities. Specific tasks highlighted the unique features of OCTOPUS, such as the exploitation of its soft arms to manipulate objects or to move in confined spaces. Our aim was to demonstrate how it is possible to combine a new generation of technologies in a unique platform through a bioinspired and biomechatronic approach. It enabled the robot to move over different terrains, pass through confined and unstructured spaces, shape its frontal arms to access narrow apertures and implement advanced grasping capabilities. All this is combined with an enhanced mechanical adaptability which translates into intrinsically safe interaction between the robot and the environment. The reported results qualify the performances of OCTOPUS and also pose new challenges and questions for the emerging field of soft robotics, in which OCTOPUS can be recognized as one of the first pioneers.

In addition, OCTOPUS has set the foundations of new soft robotics technologies, intended as the use of soft materials for robot bodyware, and it should be also considered as a sort of incubator of technologies which led to the development of new paradigms and innovative technological solutions.

Acknowledgments

This work was supported by the European Commission in the ICT-FET OCTOPUS Integrating Project,

under contract #231608 and in the ICT-FET RoboSoft Coordination Action under contract #619319.

References

- Arienti A, Calisti M, Serchi F G and Laschi C 2013 PoseiDRONE: design of a soft-bodied ROV with crawling, swimming and manipulation ability *Proc. of the MTS/IEEE OCEANS*
- Ayers J and Witting J 2007 Biomimetic approaches to the control of underwater walking machines *Trans. R. Soc. A* **365** 273–95
- Byrne R A, Kuba M J, Meisel D V, Griebel U and Mather J A 2006a Does *Octopus vulgaris* have preferred arms? *J. Comput. Psychol.* **120** 198–204
- Byrne R A, Kuba M J, Meisel D V, Griebel U and Mather J A 2006b Octopus arm choice is strongly influenced by eye use *Behav. Brain Res.* **25** 195–201
- Calisti M, Arienti A, Renda F, Levy G, Mazzolai B, Hochner B, Laschi C and Dario P 2012a Design and development of a soft robot with crawling and grasping capabilities *Proc. IEEE Int. Conf. Robotics and Automation* pp 4950–5
- Calisti M, Giorelli M and Laschi C 2012b A locomotion strategy for an octopus-bioinspired robot *Living Machines 2012 LNCS* 7375 (ed T J Prescott, N F Lepora, A Mura and Verschure PFMJ (Heidelberg: Springer) 337–8
- Calisti M, Giorelli M, Levy G, Mazzolai B, Hochner B, Laschi C and Dario P 2011 An octopus-bioinspired solution to movement and manipulation for soft robots *Bioinspir. Biomim.* **6** 036002
- Cheng N G, Lobovsky M B, Keating S J, Setapen A M, Gero K I, Hosoi A E and Iagnemma K D 2012 Design and analysis of a robust, low-cost, highly articulated manipulator enabled by jamming of granular media *IEEE Int. Conf. on Robotics and Automation* pp 4328–33
- Chen L, Armstrong C W and Raftopoulos D D 1994 An investigation on the accuracy of three-dimensional space reconstruction using the direct linear transformation technique *J. Biomech.* **27** 493–500
- Cianchetti M 2013 *Fundamentals on the Use of Shape Memory Alloys in Soft Robotics, in Interdisciplinary Mechatronics: Engineering Science and Research Development* ed M K Habib and J Paulo Davim (New York: Wiley) pp 227–54
- Cianchetti M, Arienti A, Follador M, Mazzolai B, Dario P and Laschi C 2011 Design concept and validation of a robotic arm inspired by the octopus *Mater. Sci. Eng. C* **31** 1230–9
- Cianchetti M, Licofonte A, Follador M, Rogai F and Laschi C 2014 Bioinspired soft actuation system using shape memory alloys *Actuators (Special Issue on Soft Actuators)* **3** 226–44
- Cianchetti M, Renda F, Licofonte A and Laschi C 2012 Sensorization of continuum soft robots for reconstructing their spatial configuration *Conf. Proc. IEEE on Biomedical Robotics and Biomechatronics—BioRob 2012* 634–9
- Cotton S, Olaru I M C, Bellman M, van der Ven T, Godowski J and Pratt J 2012 FastRunner: a fast, efficient and robust bipedal robot. Concept and planar simulation *Proc. IEEE Int. Conf. on Robotics and Automation* 2358–64
- Crespi A and Ijspeert A J 2008 Online optimization of swimming and crawling in an amphibious snake robot *IEEE Trans. Robot. Autom.* **24** 75–87
- Crespi A, Karakasiliotis K, Guignard A and Ijspeert A J 2013 Salamandra robotica II: an amphibious robot to study salamander-like swimming and walking gaits *IEEE Trans. Robot.* **29** 308–20
- Follador M, Cianchetti M and Laschi C 2012 Development of the functional unit of a completely soft octopus-like robotic arm *Proc. of the IEEE Int. Conf. on Biomedical Robotics and Biomechatronics (Roma, Italy)* pp 640–5
- Godage I, Nanayakkara T and Caldwell D 2012 Locomotion with continuum limbs, intelligent robots and systems (IROS) 2012 *IEEE/RSJ Int. Conf. on* pp 293–8
- Hirose S, Kikuchi H and Umetani Y 1986 The standard circular gait of a quadruped walking vehicle *Adv. Robot.* **1** 143–64

- Hou J, Bonser R H and Jeronimidis G 2012 Developing sensorized arm skin for an octopus inspired robot 2012 IEEE Int. Conf. on Robotics and Automation (ICRA) (14–18 May 2012) pp 3840–5
- Huffman C 2006 Locomotion by abdopodus aculeatus (cephalopoda: octopodidae): walking the line between primary and secondary defenses *J. Exp. Biol.* **209** 3697–707
- Kim J Y and Jun B H 2013 Design of six-legged walking robot, Little Crabster for underwater walking and operation *Adv. Robot.* **28** 77–89
- Laschi C and Cianchetti M 2014 Soft robotics: new perspectives for robot bodyware and control *Frontiers Bioeng. Biotechnol.* **2** 3
- Laschi C, Mazzolai B, Mattoli V, Cianchetti M and Dario P 2009 Design of a biomimetic robotic octopus arm *Bioinspir. Biomim.* **4** 015006
- Laschi C, Mazzolai B, Cianchetti M, Margheri L, Follador M and Dario P 2012 Soft robot arm inspired by the Octopus *Adv. Robot. (Special Issue on Soft Robotics)* **26** 709–27
- Levy G and Hochner B 2013 Coordination of flexible arms in the crawling behavior of the octopus *The Israeli Society for Neuroscience* pp 169.12/QQ23
- Levy G and Hochner B 2010 Kinematic analysis of crawling in the octopus *The Israeli Society for Neuroscience* pp poster no.430
- Li T, Nakajima K, Calisti M, Laschi C and Pfeifer R 2012 Octopus-inspired sensorimotor control of a multi-arm soft robot (ICMA) Inter. Conf. Mech. Autom. (5–8 August 2012) pp 948–55
- Lin H T, Leisk G G and Trimmer B 2011 GoQBot: a caterpillar inspired soft-bodied rolling robot *Bioinspir. Biomim.* **6** 026007
- Margheri L, Laschi C and Mazzolai B 2012 Soft robotic arm inspired by the octopus: I. From biological functions to artificial requirements *Bioinspir. Biomim.* **7** 025004
- Martinez V R, Branch L J, Fish R C, Jin L, Shepherd F R, Nunes M D R, Suo Z and Whitesides M G 2013 Robotic tentacles with three-dimensional mobility based on flexible elastomers *Adv. Mater.* **25** 205–12
- Mather J 1998 How do octopuses use their arms? *J. Comparative Psychol.* **112** 306–16
- Mazzolai B, Margheri L, Cianchetti M, Dario P and Laschi C 2012 Soft-robotic arm inspired by the octopus: II. From artificial requirements to innovative technological solutions *Bioinspir. Biomim.* **7** 025005
- Onal C and Rus D 2012 A modular approach to soft robots 2012 4th IEEE RAS EMBS Int. Conf. on Biomedical Robotics and Biomechatronics (BioRob) pp 1038–45
- Schrauwen B, Verstraeten D and Campenhout J V 2007 An overview of reservoir computing: theory, applications and implementations *Proc. of the 15th European Symp. on Artificial Neural Networks (ESANN2007)* pp 471–82
- Seok S, Onal C, Wood R, Rus D and Kim S 2010 Peristaltic locomotion with antagonistic actuators in soft robotics *Proc. of IEEE Int. Conf. on Robotics and Automation*
- Shepherd R, Ilievski F, Choi W, Morin S, Stokes A, Mazzeo A, Chen X, Wang M and Whitesides G 2011 Multigait soft robot *Proc. Natl. Acad. Sci.* **108** 20400–3
- Shim H, Jun B H, Kang H, Yoo S, Lee G M and Lee P M 2013 Development of underwater robotic arm and leg for seabed robot, CRABSTER200, OCEANS—Bergen, 2013 MTS/IEEE
- Smith K K and Kier W M 1989 Trunks, tongues and tentacles: moving with skeletons of muscle *Am. Sci.* **77** 28–35
- Steltz E, Mozeika A, Rodenberg N, Brown E and Jaeger H 2009 JSEL: jamming skin enabled locomotion *IEEE/RSJ Int. Conf. on Intelligent Robots and Systems* pp 5672–7
- Sugiyama Y and Hirai S 2004 Crawling and jumping of deformable soft robot *Proc. IEEE/RSJ Int. Conf. On Intelligent Robots and Systems* pp 3276–81
- Sumbre G, Gutfreund Y, Fiorito G, Flash T and Hochner B 2001 Control of octopus arm extension by a peripheral motor program *Science* **293** 1845–8
- Trivedi D, Rahn C D, Kier W M and Walker I D 2008 Soft robotics: biological inspiration, state of the art, and future research *Appl. Bion. Biomech.* **5** 99–117
- Walker I D 2000 Some issues in creating ‘invertebrate’ robots *Proc. of the Int. Symp. on Adaptive Motion of Animals and Machines (Montreal, Canada)*
- Walker I D 2013 Continuous backbone ‘continuum’ robot manipulators *ISRN Robot.* **2013** 1–19
- Walker I D, Dawson D, Flash T, Grasso F, Hanlon R, Hochner B, Kier W, Pagano C, Rahn C and Zhang Q 2005 Continuum robot arms inspired by cephalopods *Proc. SPIE Conf. Unmanned Ground Veh. Tech. (Orlando, FL)* pp 303–14
- Walker I D, Mattfeld R, Mutlu A, Bartow A and Giri N 2012 A novel approach to robotic climbing using continuum appendages in in-situ exploration *IEEE Aerospace Conf.* 1–10
- Webster R J III and Jones B A 2010 Design and kinematic modeling of constant curvature continuum robots: a review *Intern. J. of Robot. Res.* **29** 1661–83
- Wells M J 1978 *Octopus. Physiology and Behaviour of an Advanced Invertebrate* (London: Chapman and Hall)